Lab on a Chip

SIZE AND DENSITY MEASUREMENTS OF SINGLE SICKLE RED BLOOD CELLS USING MICROFLUIDIC MAGNETIC LEVITATION

Journal:	*Lab on a Chip*
Manuscript ID	LC-ART-08-2021-000686.R1
Article Type:	Paper
Date Submitted by the Author:	20-Dec-2021
Complete List of Authors:	Goreke, Utku; Case Western Reserve University, Mechanical & Aerospace Engineering Bode, Allison; Case Western Reserve University Yaman, Sena; Stanford University Gurkan, Umut; Case Western Reserve University, Mechanical and Aerospace Engineering Durmus, Naside Gozde; Stanford University,

SIZE AND DENSITY MEASUREMENTS OF SINGLE SICKLE RED BLOOD CELLS USING MICROFLUIDIC MAGNETIC LEVITATION

Utku Goreke,[1] Allison Bode,[1,2] Sena Yaman,[4] Umut A. Gurkan,[1,3*] Naside Gozde Durmus[4*]

[1]Department of Mechanical and Aerospace Engineering, Case Western Reserve University, Cleveland, OH, USA
[2]Department of Hematology and Oncology, School of Medicine, Case Western Reserve University, Cleveland, OH, USA
[3]Department of Biomedical Engineering, Case Western Reserve University, Cleveland, OH, USA
[4]Molecular Imaging Program at Stanford (MIPS), Department of Radiology, Stanford University, Stanford, CA, USA

***Corresponding Authors:**
Umut A. Gurkan, Ph.D.
Warren E. Rupp Associate Professor
Mechanical and Aerospace Engineering
Biomedical Engineering
Case Western Reserve University
umut@case.edu

Naside Gozde Durmus, Ph.D.
Assistant Professor
Department of Radiology
Molecular Imaging Program at Stanford (MIPS)
Stanford University School of Medicine
3165 Porter Drive, Palo Alto, CA 94304
gdurmus@stanford.edu

This research was, in part, funded by the National Institutes of Health (NIH) Agreement OT2HL152643. The views and conclusions contained in this document are those of the authors and should not be interpreted as representing the official policies, either expressed or implied, of the NIH.

ABSTRACT

Single cells have unique biophysical signatures that can rapidly change during various healthy and pathological states. For instance, cellular density is an inherent property differing between cell types. Characterizing dramatic changes in fundamental density properties down to the single-cell level can reveal sub-populations in pathological states. Here, we have developed a microfluidic, magnetic levitation-based assay (MagDense) that detects minute density differences of individual red blood cells (RBCs) down to 0.0001 g/mL resolution. This assay fractionates RBCs based on their density profiles in a non-ionic paramagnetic medium flowing in a capillary microchannel placed between magnets with same poles facing each other. Based on precisely measured levitation height and density of individual RBCs at their specific equilibrium state, we demonstrated that MagDense can accurately analyze the density of HbS-containing RBCs and HbA-containing RBCs. In addition, the precise density and cell size measurements at the single cell level showed three different sub-populations of RBCs in blood samples from individuals with homozygous sickle cell disease receiving blood transfusions; where less dense, HbA-containing RBCs levitated higher, while the denser, HbS-containing RBCs levitated lower. We compared the mean RBC densities of sickle cell disease subjects with non-sickle controls and found distinctly separated density bands of RBC density for each group denoting likely range of cell densities seen in the blood samples. High resolution of our method enabled measurement of deviation from the mean RBC density. Moreover, we introduced a new term as a measure of density dispersion, “RBC Levitational Density Width, RLDW”. Mean RBC density in sickle cell disease associated with hemoglobin from complete blood count ($p=0.032$, Linear regression) and RLDW associated with absolute reticulocyte count (ARC) and RBC distribution width (RDW) from complete blood count ($p=0.002$ for ARC and $p=003$ for RDW, Linear regression). Our magnetic levitation-based assay enables rapid, accurate, density-based imaging, profiling and label-free monitoring of single RBCs. Our approach can be broadly applicable to investigate blood cell disorders and the effects of emerging curative therapies in patient outcomes.

Keywords

Biophysics, cytometry, magnetic levitation, single-cell density, sickle cell disease (SCD)

INTRODUCTION

Sickle cell disease (SCD) is an inherited disease which afflicts millions of people worldwide and is associated with vaso-occlusion, ischemia, and inflammation with considerable morbidity and early mortality.[1, 2] During painful vaso-occlusive crises in SCD, there is a significant intravascular activation of the immune system that leads to complement deposition on red blood cell (RBC) membranes, triggering profound metabolic changes in circulating RBCs, leading to increased cell density and changes in RBC biophysical properties.[3, 4] The pathophysiology of SCD is a consequence of abnormal polymerization of deoxygenated sickle hemoglobin (HbS).[5, 6] HbS polymerization may result in RBC dehydration and subsequent RBC density increase, via increased cation permeability due to activation of transport mechanisms such as the Na+/K+/2Cl- cotransporter 1 ([NKCC1]), Gardos channels and Psickle channels.[7-10] Rapid HbS polymerization is inversely proportional to intracellular concentration of HbS,[11] therefore increased cell density due to loss of water catalyzes the HbS polymerization.

RBC density is a physical property with clinical implications in SCD. Sickle RBCs (sRBCs) have an overall increased average cell density,[12, 13] however, the density of sRBCs varies at the single cell level. A fraction of sRBCs share the same density as normal RBCs of the same circulation age, though the majority of sRBCs show a significantly increased density even under normoxic conditions. All types of RBCs undergo dehydration stochastically[14] therefore, density distribution of red blood cells varies widely between individual patients.[15] For instance, a broader RBC density distribution in individuals with SCD and concomitant α-thalassemia is associated with less severe SCD phenotype.[15] Furthermore, higher RBC density is reported to be associated with elevated hemolysis and comorbidities such as skin ulcers, renal failure and priapism.[15] In addition, murine models have shown that vascular occlusion may be initiated by a small number of dense RBCs[16], which is consistent with reports of increased presence of dense red blood cells in individuals with SCD during painful vaso-occlusive crises.[17]

Currently, assessment of red blood cell density in SCD is performed with density fractionation methods, such as aqueous multiphase systems, arabinogalactan density gradient, and phthalate density-distribution.[15, 17, 18] However, the resolution of these methods are ultimately limited with the number of immiscible phases. For example, Ficoll gradient centrifugation separates red blood cells in a liquid density/concentration gradient. This method can be used to estimate the “average” density of the RBC population. However, it does not allow for accurate density measurements or assessment of the heterogeneity of RBCs at the single-cell level. It also requires a priori knowledge of cell density, thus, unbiased measurements cannot be ascertained. In addition, exposure to the concentrated solutions of substances used to construct the density gradient may inadvertently affect the density and viability of cells.[19] There have been a few methods established to measure the density of single cells with high precision. Nanomechanical resonators[20] allow measurement of cellular density, however they require measurements in two separate fluids with known densities in a vacuum-packaged micro-cantilever that prevents real-time imaging and monitoring of the dynamic cellular changes in RBCs.[21, 22] Although the heterogeneity of RBC density is associated with significant clinical outcomes in SCD, a fine resolution assessment of red blood cell density which is accessible and clinically meaningful has not yet been achieved due to these technical challenges. The lack of precise measurements of single cells and clinical correlates for the red blood cell distribution hindered the assessment of potential additional indications. Precise

identification of single red blood cell density heterogeneity and understanding of intercellular variability within homogenous or mixed red blood cell populations is essential for monitoring SCD state during therapeutic interventions and emerging curative therapies, to fully evaluate the impact of these treatments on patient outcomes.[23]

Here, we have developed a microfluidic, magnetic levitation-based assay (MagDense) that can detect minute density differences of single red blood cells (RBCs) and investigate their heterogeneity with 0.0001 g/mL sensitivity. Although we and others previously demonstrated that cells can be levitated to varying heights under a magnetic field, the applications of magnetic levitation to investigate the heterogeneity and density distribution of individual RBCs in SCD has not been presented yet. Magnetic levitation-based assay fractionates single RBCs based on their density profiles in a non-ionic paramagnetic medium flowing in a capillary microchannel placed between magnets with same poles facing each other. The system captures microscopic images of single RBCs as they flow in the microchannel in a levitated state. To measure the density distribution of individual RBCs with high sensitivity and high throughput, we performed automated image analysis which extracts quantitative measures of RBC levitation heights and cell size, and converts the levitation signatures into density information for each cell. Based on precisely measured levitation heights and density of single RBCs in their levitated state, we demonstrated that MagDense can accurately analyze the density of HbS-containing RBCs and HbA-containing RBCs. In addition, we showed that the differences in cell density promoted by abnormal metabolism of sickle RBCs can be clearly detected in the magnetic levitation device. Furthermore, our precise density and cell size measurements at the single cell level showed three different sub-populations of RBCs in transfused SCD (HbSS) blood sample, where less dense HbA-containing RBCs levitated higher, while the denser HbS-containing RBCs levitated lower and elongated and dense RBCs clustered during post-processing. Our clustering analysis approach based on size and density of individual RBCs adds to the existing knowledge on dense RBCs in the context of SCD. Magnetic levitation-based assay enables rapid, accurate, density-based imaging, profiling and label-free monitoring single RBCs.

RESULTS

Magnetic Levitation Platform Design and Development

The levitation channel of the MagDense platform has a 1mm × 1mm cross-sectional area, a length of 50 mm and a wall thickness of 0.2 mm (**Figure 1A**). The light path of the microscope traverses through the channel in the horizontal direction (**Figure 1A**) with two mirrors that are placed at a 45° angle. The channel is structurally fixed between two magnets with 1.40 T of internal flux density (**Figure 1A**). Red blood cells equilibrate in a non-toxic, non-ionic paramagnetic medium (Gd, Gadavist), which is a Food and Drug Agency-approved magnetic resonance imaging contrast agent (**Figure 1B**). The paramagnetic medium overshadows the possible interference due to magnetic susceptibility of the red blood cells.[24] The magnitude of the magnetic force, F_{mag}, depends on the distance from the magnets,[25-27] while the magnitude of the gravitational force, F_g, depends on the density of the red blood cells in the channel (**Figure 1B**). F_g always acts on the red blood cells towards the bottom of the channel since we use 30 mM paramagnetic medium with a density of 1.0208 g/ml; which is below the range of expected red blood cell density.[22] As a result of this unique magnetic design and configuration, these two forces, F_{mag} and F_g, act in the same

direction in the upper half of the channel, while they act in opposite directions in the lower half of the channel. Once the system reaches equilibrium, i.e., $F_{mag}=F_g$, all the red blood cells levitate in the bottom half of the channel at a height, based on the density of each single cell, independent of their volume or shape (Supplementary Figure 1-2).[28-30] The separation distance between the cells can be modified by changing the height of the channel (Supplementary Figure 3). Sickle red blood cells with abnormal densities levitate closer to the bottom magnet indicating a higher cell density (**Figure 1B-C**). In addition, the cells are focused in the transverse axis, where the magnetic induction strength in the transverse direction is negligible, therefore a single image capture along the capillary is sufficient to capture the heights of all the red blood cells after equilibrium (**Figure 1D-E**). Thus, red blood cells with various densities and different sizes can be analyzed without changing the design of the magnetic levitation platform. (*Detailed information on the underlying physics of magnetic levitation is provided in the Supplementary Information*).

Testing and Validation of Platform with Beads of Known Densities

We validated the functionality, accuracy and precision of the MagDense platform using polyethylene beads (Cospheric) with known densities. Our experimental design included 1.025 to 1.130 g/ml reference beads, representing the density ranges of HbAA and HbSS RBCs, as reported in the literature[15] (**Supplementary Figure 4**). Corresponding beads were suspended in a 1X phosphate buffered saline (PBS) with 30 mM paramagnetic solution and then were introduced into the levitation channel. Within ten seconds, several hundred beads equilibrated and levitated at different heights, based on their individual densities (**Figure 1F**). Fitting the resulting plot of density (g/mL) vs. levitation height (μm) to a linear curve provided a standard function to measure densities. Linear fitting of the average heights of each bead group exhibited excellent goodness-of-fit (**Figure 1G**, Adjusted R^2=0.97). The slope of the linear fit was 3.08×10^{-4} g/ml/μm. Considering the single pixel size that can be attained under a 20x objective is 0.317 μm, this slope value resulted in a density measurement resolution of 0.98×10^{-4} g/ml/pixel.

Magnetic Levitation-based Morphology and Density Profiling of Single RBCs

Next, to demonstrate our capability to characterize RBCs at the individual cell level, we levitated and measured the RBC densities of an adult non-sickle control subject (HbAA) and an adult subject with SCD (**Figure 2, Supplementary Videos 1-3**). Densities of several hundred cells (N=113 for HbAA, N=270 for HbSS hydroxyurea, N=493 for HbSS post-hematopoietic stem cell transplantation (HSTC)) were rapidly measured individually, producing a histogram graph of density distribution of individual RBCs (**Figure 2A**). According to the density measurements at the single cell level, the HbSS RBCs were more heterogeneously distributed compared to the HbAA RBCs (**Figure 2A**, SD=0.009 g/ml for HbSS hydroxyurea (red), SD=0.005 g/ml for HU HbSS (purple), SD=0.004 g/ml for HbAA (blue)). A second dimension was added to these histogram plots with RBC size (major axis length) information of individual cells, converting the histograms into scatter plots (**Figure 2B**). The sizes of 95% confidence ellipses of three samples demonstrate an inverse relationship with HbA%. Notably, we observed heterogeneity within each seemingly homogenous cell red blood population.

Clustering Analysis of Sickle Red Blood Cells Based On Morphology and Density

We further analyzed the scatter plots generated by simultaneous size and density measurements at the single cell level by clustering methods. Major groups of RBCs in SCD were classified as light and dense discocytes, which retain their discoid shapes in normoxic conditions and irreversibly

sickled cells (ISCs) based on literature.[7] These three clusters of RBCs were identified by bottom-up clustering analysis (**Figure 3**). Several RBCs were depicted as inset figures next to their corresponding dots. Group 1 (green, N=298) which consisted of HbAA RBCs and light discocytes represented the most of the RBCs in these clusters. Interestingly, we found that more than half (17/32) of the RBCs that have densities greater than 1.118 g/ml were not classified as ISCs. These results demonstrate the feasibility of single cell density and morphology characterization of red blood cells with MagDense platform.

RBC Density as an Indicator of SCD

Next, we assessed the RBC densities of adult subjects with SCD (N=16) and healthy adult subjects with no known hemoglobinopathies as control (N=12). The density of HbSS RBCs from subjects with SCD was shown to be significantly higher compared to HbAA RBCs in control group (**Figure 4A**, HbSS: N = 16, mean ± SD = 1.110 ± 0.011, and HbAA: N = 12, mean ± SD = 1.089 ± 0.007, one-way ANOVA, $p<0.001$). The age range for the subjects were 18-40 years old for both groups. We defined an HbSS (rose color) and HbAA band (light blue color) based on the interquartile ranges of each group indicating the likely range of cell densities seen in the blood samples. These bands were between 1.085 and 1.093 g/ml for non-sickle control subjects and 1.102 and 1.119 g/ml for SCD subjects. Notably, the density of red blood cells from two SCD subjects fell on the border of the HbAA band, while the density of cells from one non-sickle control subject was borderline on the HbSS band. Of note, microscope images that were used for the analysis were shown for HbAA sample (**Figure 4A(*i-ii*)**) and for HbSS samples (**Figure 4A(*iii-iv*)**). The median density values which are defined as "D50" in the previous literature[15] were found as 1.110±0.011g/ml (mean±SD) (**Supplementary Table 1**). In addition, we analyzed the ability of MagDense platform in differentiating between hemoglobin types based on RBC density by plotting receiver operating characteristic curve (ROC curve) (**Figure 4B**). ROC curve plots the true positive rate (sensitivity) with false positive rate (1-specificity) at varying thresholds to illustrate the diagnostic ability of a device. The point at which sensitivity and 1-specificity are unity denotes the perfect diagnostic device, while the line at which sensitivity equals 1-specificity denotes a random guess. The further the ROC curve from the random guess line towards the perfect diagnosis point the better the diagnostic ability of the device. ROC output for different thresholds was shown in **Figure 4C**. The minimum accuracy associated with these thresholds was 85.7% and the minimum distance to the unity was achieved at the threshold of 1.100 g/ml. These results demonstrate the ability of the MagDense to discriminate among hemoglobin types and suggest that RBC density is useful as an indicator of SCD.

RBC Levitational Density Width as a New Biophysical Parameter

Next, we investigated the distribution patterns of RBCs within the MagDense platform. The density distribution of HbSS RBCs was wider compared to HbAA RBCs, and the RBC density distributions of individual patients were significantly different from each other in each group (**Figure 5A**). The standard deviation of the averaged RBC density curves was greater in HbSS compared to HbAA ((**Figure 5A**, 0.014 vs 0.011). Therefore, we decided to parametrize the dispersion of RBC density distribution. We defined the new RBC density parameter, "RBC Levitational Density Width (RLDW)", as:

$$RLDW = \left(\frac{Weighted\ standard\ deviation\ of\ RBC\ density\ distribution}{Mean\ RBC\ density}\right) \times 100 \qquad (1)$$

The definition of RLDW is similar to the "RBC distribution width (RDW)", which is a standard complete blood count output that describes the dispersion of mean corpuscular volume (MCV). RLDW reflects the dispersion of RBC density within the MagDense device. Collectively, our results suggest that RBC density distribution can be described with two independent parameters; mean RBC density and RLDW.

Clinical Associations of Density Distribution Parameters

The complete blood count (CBC) was performed for subjects with SCD on the day of their visit to the clinic, therefore these CBC results reflect the characteristic of the samples used in this study for the SCD subjects group. We analyzed CBC results and sought systematically whether there is a relation with HbSS RBCs density parameters. Since CBC was not performed for the HbAA samples in this study, we found it appropriate to show the reference ranges of CBC parameters for HbAA subjects where the data is expected to be seen on the plots.[31-33] These reference ranges are annotated with blue bounding boxes in **Figure 6A-D**. We found a significant association between hemoglobin concentration (Hbg) and mean RBC density for HbSS RBCs (**Figure 6A**, PCC=0.54, p=0.032, Pearson correlation and linear regression). Hemoglobin accounts for considerable portion of overall RBC mass, therefore although there are other factors affecting the cellular density such as hydration status of the cells, the hemoglobin content of RBCs could be indicative of cellular density for RBCs. Elevated absolute reticulocyte count (ARC) is a consequence of severe anemia in SCD because the reticulocytosis is enhanced to compensate the low RBC levels. Therefore, we investigated the association between ARC and the density distribution parameters; mean RBC density and RLDW. We found no significant association of ARC with mean RBC density (Figure 6B, PCC = 0.37 and p=0.156, Pearson correlation and linear regression). However, the elevated ARC levels were significantly related to increased RLDW (**Figure 6C**, PCC = 0.69 and p=0.003, Pearson correlation and linear regression). RBC size distribution dispersion is characterized by RDW in CBC. RDW describes the dispersion of cell volume from the mean and RLDW is defined in a similar manner with RDW. We found a significant association between RDW and RLDW (**Figure 6D**, PCC = 0.70 and p=0.002, Pearson correlation and linear regression).

Red Blood Cell Density as a Treatment Response Measure in SCD

We assessed the RBC densities of three individuals with SCD before and after the subjects receive different treatments; blood transfusion and hematopoietic stem cell transplantation (HSCT). Transfusions are desperately needed for some SCD subjects and they are shown to have positive effects on morbidity and mortality in SCD. When SCD patients receive transfusion, their blood is replaced either partially or fully with a non-sickle blood containing HbAA RBCs. Two subjects received partial exchange transfusion, which increased HbA percentage. The subsequent increase in levitation height of RBCs can be visually observed in microscope images of MagDense capillary (**Figure 7A-B**). Post-treatment RBC density profiles for both subjects approached to HbAA band from HbSS band (**Figure 7C-D**). For one of the subjects, the HbA percentage from 1.9% to 29.4% and the RLDW of the distribution increased after the subject received transfusion treatment (0.71% vs 0.99%). For the second subject, the HbA percentage from 62.3% to 80.1% and the RLDW of the distribution decreased (1.14% vs 0.66%). Additionally, a similar change in levitational height is observed following a HSCT of another HbSS SCD subject (**Figure 7E**). HSCT is a curative therapy where a bone marrow is transplanted to the SCD subject. Before the HSCT, the subject received a transfusion and the HbA percentage is increased. The mean RBC density was decreased

(from 1.124 g/ml to 1.107 g/ml) and RLDW was increased (from 0.33% to 1.02%) following a curative therapy (**Figure 7F**).

DISCUSSION

RBC density in SCD has attracted considerable attention in the field, especially due to the vicious feedback loop between activated dehydration pathways and hemoglobin polymerization. However, significant limitations of the existing RBC density measurement methods hindered the widespread and precise evaluation of RBC density in clinical settings. Here, we presented RBC density measurements in SCD with the MagDense platform, which can achieve precise, high throughput, label-free density assessment at the single RBC level. Complementary size measurements of sickle red blood cells enabled accurate assessment of dense and elongated ISCs. We determined the heterogeneity and density parameters of HbS and HbA containing RBCs with unprecedented resolution.

Fractionation with multiphase emulsions is the most widespread RBC density assessment method but these methods only provide coarse assessment of red blood cell density. For example, the ADVIA hematology analyzer can only make a binary classification of red blood cells by density.[34] Although utilized commonly in clinical studies, fractionation methods sacrifice resolution by clustering RBCs with similar densities between preset thresholds, but these preset thresholds for RBC density bound the range that can be attained, therefore the true density range information cannot be definitively resolved. Even the most advanced density fractionation methods that are being used in other pioneering clinical research can classify the cells into only 12 groups.[23] MagDense platform is a miniaturized alternative to the fractionation methods with significant advantages. Firstly, a continuous density gradient generated across the paramagnetic medium allows continuous resolution of density (**Figure 1F-G**). Secondly, MagDense can provide a minimum resolvable density change of 0.0001 g/ml as we demonstrated by levitating microbeads with precisely known densities (**Figure 1G, Supplementary Figure 4**). Finally, microscope images of the capillary can be post-processed to obtain further information about the red blood cells (i.e., size). As we demonstrated, this advantage adds a unique value to MagDense and facilitates simultaneous RBC density and size analysis at a single cell level (**Figure 2-3**). Fractionation methods achieve density separation with centrifugation, and it is often difficult to post-process the sample. Taken together, these advantages highlight the usefulness of the MagDense platform as a greatly reduced scale alternative to the existing methods for measurement of density parameters of RBCs in SCD.

Although the number of SCD subjects may be considered low in our study, we measured the densities of several hundred RBCs individually for each subject. Since the MagDense platform does not require preset thresholds and can attain high resolution, we independently determined the previously undefined range of HbSS as well as HbAA RBC density in a statistically powerful manner (**Figure 4-5**). We defined HbAA and HbSS bands based on the quartiles of mean RBC density of non-sickle control and SCD subjects (**Figure 4A**). The actual ranges of mean RBC density were between 1.078 g/ml - 1.102 g/ml for non-sickle controls and 1.093g/ml-1.128 g/ml for SCD subjects (**Figure 4A**). These results substantiate previous findings in the literature.[7, 15, 35] The study with the largest known cohort to date for RBC density in SCD, described RBCs with densities greater than 1.12 g/ml density as dense RBCs and reported the mean of dense RBC

percentage as 12.7%. In comparison, we found percentage of dense RBCs as 23.9% (**Supplementary Table 1**). Considering the differences in measurement methods and patient cohorts, this difference can be regarded as a rather acceptable difference. Additionally, although the ranges of mean RBC density associated with the two groups overlapped, the receiver-operating curve for distinguishing HbSS from HbAA samples demonstrated decent specificity for the MagDense platform (**Figure 4B-C**).

We observed notable inter-subject heterogeneity of mean RBC densities in the SCD blood samples (**Figure 4A**, SD=0.011). The samples were collected from SCD patients at their clinical baseline and we found no association of mean RBC density with pain level reported by the subject at their outpatient visit the same day (p=0.99, Linear regression, data not shown). The wide range of SCD mean RBC densities measured in the MagDense system could be due to the intricate nature of SCD phenotypes, as illustrated by others as well.[15, 36, 37] For example, higher HbF percentage is shown to be associated with less dense RBCs in SCD patients in general,[34, 38] and attenuated HbS polymerization,[39] although HbF percentage has little effect on RBC dehydration[40] and is shown to be unassociated with RBC density in some subphenotypes.[15] Furthermore, presence of concurrent SCD and α-thalassemia deletions was associated with an overall less dense RBC profile.[15, 36, 37, 41] More specifically, α-thalassemia may regulate the fraction of RBCs that achieve high cell density in SCD,[41] possibly through downregulation of genes including the Gardos channel (KCNN4) and K-Cl cotransporter (KCC1).[42] The interplay of these disease variables could explain the high heterogeneity of average RBC densities we observed and why RBC density for two of the SCD subjects in our cohort fell close to HbAA band. Non-sickle control subjects also demonstrated inter-subject heterogeneity as implicated by noteworthy dispersion (SD=0.007). In fact, mean RBC density values of two control subjects were close to the lower boundary of the HbSS band and were higher than those of three SCD subjects (**Figure 4A**).

Heterogeneity was also present in single and averaged RBC density distribution curves (**Figure 5A)** suggesting intra-subject RBC density heterogeneity. Our group and others have reported heterogeneous RBC biophysical properties in SCD. To evaluate the intra-subject RBC density heterogeneity, we coined a new term 'RLDW'. Similar to an established CBC panel term, Red Cell Distribution Width(RDW), RLDW is a measure of mean normalized dispersion of the RBC density per sample whereas RDW is a measure of mean normalized dispersion of the RBC size. We postulated that it would be clinically meaningful to describe RBC density with these two parameters: RLDW and mean RBC density. Next, we investigated the clinical associations of these two density parameters. Mean RBC density in SCD blood samples was associated with hemoglobin concentration (Hbg, **Figure 6A**). Although hemoglobin constitutes a large portion of the RBC mass, some intracellular hemoglobin is lost within the bloodstream in SCD. Hemoglobin concentration from a CBC panel includes both intracellular and extracellular hemoglobin, but we could not find a correlation between mean corpuscular hemoglobin concentration and mean RBC density (MCHC, data not shown, PCC = 0.07 and p=0.797, Pearson correlation and linear regression). This lack of association is hardly surprising because MCHC is measured from RBC lysate, not from intact RBCs. Therefore, MCHC may not reflect the true intracellular hemoglobin concentration in SCD patients who have extracellular hemoglobin. It should also be noted that cellular hemoglobin concentration mean (CHCM) index which is optically estimated from intact RBCs was not reported in the CBC panel. While we could not find any other significant relationship between mean RBC density and other central laboratory test results, RLDW strongly

associated with two clinical indices: ARC and RLDW (**Figure 6C-D**). ARC is an index of the bone marrow's response to hemolysis and it could be several times greater in SCD patients than that of adults with no hemoglobinopathy. ARC provides crucial information on the anemia status of the patient. Quinn et al. successfully provided plausible evidence for a strong inverse relationship between mean RBC survival and ARC in SCD.[43] Increased number of reticulocytes which have lower density compared to mature erythrocytes could cause elevated intra-subject heterogeneity of RBC density distribution as measured by RLDW. Regarding RDW, it is an index of RBC volume variation and it is elevated in SCD due to the misshapen RBCs. RDW has multiple clinical applications and is an adverse prognostic factor in many diseases.[44-47] Association between RDW and RLDW can be also be attributed to the elevated number of reticulocytes which have larger than average MCV or irreversibly sickled RBCs which are both elongated and highly dense. Unlike RDW, the ranges of RLDW for HbAA and HbSS samples were similar (**Figure 6D**).

Successful treatment could modify the mean RBC density in SCD. Treatments that aim to reverse the underlying pathophysiology by delaying or disrupting the polymerization of HbS currently include hydroxyurea, transfusion, and allogeneic HSCT. Curative gene therapies to correct the βs point mutation is currently under investigation and these studies utilize RBC density measurements with density fractionation methods.[23, 48] RBC density in SCD is considered a steady disease parameter without known clinical intervention options.[37] Here, we demonstrate that our MagDense platform can assess the treatment response by measuring the RBC density precisely. After two SCD subjects received transfusion therapy and after another SCD subject received HSCT, the mean RBC density migrated from the HbSS to the HbAA band (**Figure 7**). In these cases, RLDW was greater when the HbA percentage was closer to 50%. We postulate that high resolution RBC density assessment via MagDense could be used for assessing treatment response to curative therapies in SCD.

We note that our study has some possible limitations. One limitation is the variability of the levitation height results that may arise from manual steps in the image analysis process. While our image analysis algorithm is automated, each user needs to semi-manually set the parameters to define the top and bottom levitation channel boundaries. Small variations in image analysis can be eliminated by introducing beads with a known density in the levitation media, which will act as a reference point in every measurement, and will ensure the accuracy and repeatability, and eliminate any user-to-user variability.[49] Another limitation for magnetic levitation of the RBCs arises due to the variation of magnetic susceptibilities of hemoglobin molecules. The MagDense platform levitates the cells by leveraging the magnetic susceptibility difference between the medium (χ_m) and the cells (χ_c) . In our method, the magnetic susceptibility variation of hemoglobins is very small with respect to the large magnetic susceptibility of the paramagnetic medium. Therefore, we neglected the variation in the magnetic susceptibility of hemoglobins and assumed the same χ_m for all RBCs. Another concern may arise from the use of gadolinium-based contrast agents (i.e. Gadavist) due to its possible influence on cell viability. Gadavist is an FDA-approved, human-injectable, non-toxic MRI imaging contrast agent and is used for generating large χ_m in the MagDense platform. In our earlier studies, we showed that paramagnetic medium did not affect the viability and proliferation rate of cells over 5 days.[30, 50, 51] In a small clinical study, *in vivo* treatment with gadolinium-based contrast agents do not appear to be associated with increased risk of vaso-occlusive or hemolytic adverse events when administered to the SCD

patients.[52] We consider the possible effects of these limitations to be negligible on the performance of the MagDense platform.

CONCLUSIONS

Investigation of the mechanism of increases in RBC density in SCD must be considered work in progress. RBC density is associated with specific clinical manifestations and biologic markers and may be a useful addition to the biologic and clinical evaluation of patients with SCD. In addition, RBC density is considered a steady disease parameter in the absence of clinical interventions,[35] which makes it highly suitable for monitoring disease status. Our technique has a great potential to advance our understanding of disorders and diseases that affect RBC density and to be used as a companion diagnostic device to determine efficacy of a treatment of a specific patient. On the outlook, we plan to standardize MagDense assay for widespread use in SCD and make it broadly applicable to investigate blood cell disorders and emerging curative therapies in patient outcomes.

CONFLICTS OF INTEREST

N.G.D is a co-founder of and has an equity interest in Levitas Bio, Inc., a company that develops new biotechnology tools for cell sorting and diagnostics. Her interests were viewed and managed in accordance with the conflict of interest policies. U.A.G. and Case Western Reserve University have financial interests in Hemex Health Inc. U.A.G. and Case Western Reserve University have financial interests in BioChip Labs Inc. U.A.G. and Case Western Reserve University have financial interests in Xatek Inc. U.A.G. has financial interests in DxNow Inc. Financial interests include licensed intellectual property, stock ownership, research funding, employment, and consulting. Hemex Health Inc. offers point-of-care diagnostics for hemoglobin disorders, anemia, and malaria. BioChip Labs Inc. offers commercial clinical microfluidic biomarker assays for inherited or acquired blood disorders. Xatek Inc. offers point-of-care global assays to evaluate the hemostatic process. DxNow Inc. offers microfluidic and bio-imaging technologies for *in vitro* fertilization, forensics, and diagnostics. Competing interests of Case Western Reserve University employees are overseen and managed by the Conflict of Interests Committee according to a Conflict-of-Interest Management Plan.

ACKNOWLEDGEMENTS

N.G.D. acknowledges support from the Career Award at the Scientific Interface (CASI) from the Burroughs Wellcome Foundation (BWF). N.G.D. also acknowledges funding from McCormick and Gabilan Faculty Award from Stanford University, the Donald E. and Delia B. Baxter Foundation and Koret Foundation. This research was, in part, funded by the National Institutes of Health (NIH) Agreement OT2HL152643. U.A.G acknowledges the support from National Heart Lung and Blood Institute (NHLBI) R01HL133574. U.A.G also acknowledges the support from National Science Foundation (NSF) Career Award 1552782. The views and conclusions contained in this document are those of the authors and should not be interpreted as representing the official policies, either expressed or implied, of the NIH.

MATERIALS AND METHODS

Fabrication of MagDense Platform: A magnetic levitation device (MagDense) makes up the sample processing unit. It consists of custom-made polymethyl methacrylate (PMMA), permanent neodymium magnets, and mirrors. The samples were loaded into to a glass microcapillary channel (Supplementary Figure 5) which was placed between two N52-grade neodymium magnets (NdFeB, 50mm in length, 2mm in width, and 5 mm in height) which were oriented with the same poles facing each other. For high-resolution real-time imaging purposes, two mirrors were placed at each side of the microchannel. For levitation experiments, a paramagnetic medium was used: red blood cells/particles were spiked in a non-ionic gadolinium-based paramagnetic medium (i.e., Gadavist). Paramagnetic medium was aliquoted upon receipt and freshly prepared paramagnetic medium was used in each experiment. The levitation chip can be placed under either a 5X, 10X or 20X objective on the microscope and the levitation profiles of objects (i.e., polystyrene beads, red blood cells) can be imaged and recorded.

Image Analysis of Levitated Sickle RBCs: Image analysis and characterization of levitation profiles for red blood cells were performed using a customized in-house developed code, employing the Image Processing toolbox in MATLAB. The image datasets were acquired using the ZenPro2 software (Zeiss) and were imported into the code in *.tiff* format. Collected cell levitation images were imported as RGB images from the source *.tiff* file and were converted to grayscale. Gaussian smoothing was applied to remove high-frequency noise from the image, followed by a Laplacian operation to filter low-frequency noise. The image was then binarized, generating an image that identified only the cell positive pixels. Pixel values were then summed across rows, and the array was reversed. Thus, 0 corresponds to the bottom of the capillary channel (0 μm) and 1,000 (1,000 μm) corresponds to the top. These values were summed, with indices counted, to generate a list of levitation heights for all cell-positive pixels. The results were plotted to analyze the distribution of the heights of all cell-containing pixels.

To accurately image individual RBCs in MagDense, the whole blood samples from HbAA and HbSS subjects were diluted at a 1:10,000 ratio and then were levitated in PBS with 30 mM paramagnetic medium. RBCs were equilibrated at unique levitation heights within twenty minutes for both samples. Individual RBC sizes were recognized from the microscope images using count tool of Adobe Photoshop CC© along with an in-house developed JavaScript algorithm that targets Adobe Photoshop CC to extract the pixel locations of count objects. More specifically, count objects were placed manually on each end of the cells and then the major axis length was calculated from the distance between two consecutive count object locations. This method allows discerning the levitating cells with accuracy as long as the two most distant ends of the cells are visible, even when the cells overlap, since this approach does not involve computer vision.

System Calibration for Levitation Experiments: Microbeads with known densities (Cospheric) were used to determine the accuracy and precision of the density measurements performed in the magnetic levitation device. The system was calibrated with reference microbeads having known densities (i.e., 1.025 g/mL, 1.030 g/mL, 1.050 g/mL, 1.089 g/mL, 1.13 g/mL) to generate a standard curve that correlated “the levitation height of RBC” to “the density of RBC”. Each of the reference bead solutions were levitated in a 30 mM paramagnetic medium and beads were imaged at their equilibrium height. Fitting the resulting plot of density (g/mL) vs. levitation height (μm) to a linear curve provided a standard function to measure densities. Based on these curves, the

resolution and dynamic range of density measurements for the MagDense platform were calculated. Our algorithm allows rapid, high-throughput analysis of levitation measurements and eliminates user to user bias of manual counting, enhancing the reproducibility of the levitation-based density measurements. Moreover, to investigate the effect of particle shape on levitation height, non-spherical, 4 μm polystyrene particles with same density and with various shapes (i.e., peanut and snowman) (Magsphere, Inc) were re-suspended in PBS and levitated at 30 mM paramagnetic medium.

Processing and Magnetic Levitation of Sickle Cell Patient Whole Blood Samples: Blood samples from subjects with SCD and non-sickle control were obtained via standard laboratory procedures approved by the IRB. Clinical information, including medical history and treatment course, and blood samples were collected after patients had provided informed consent. Upon collection, the samples were treated with an anticoagulant, EDTA, in vacutainer tubes, and were stored at 4°C. Blood samples were shipped overnight on ice for the assessment of RBC density. Samples were received within 24 hours from the time of collection and density analysis was performed immediately upon receipt. Upon arrival, the samples were maintained at a temperature between 2-8°C. For levitation experiments, whole blood was diluted at 1:10,000 and 1:100,000 ratios with phosphate buffered saline (PBS). A 30-microliter blood sample was prepared with non-ionic, non-cytotoxic paramagnetic medium (Gadolinium) and injected into the microcapillary via a pipette. The microcapillary was then sealed on both ends with Critoseal to contain the sample. The levitation height pattern was then imaged once the cells reached their equilibrium, which took approximately 20 minutes for RBCs under the protocol conditions used for the experiments outlined here.

Subjects: All subjects in this study had phenotypic homozygous sickle hemoglobin (HbSS or HbSβ0) and were at their clinical baseline at the time of sample collection. Samples and data were collected under an Institutional Review Board approved protocol (registered at *www.clinicaltrials.gov* as #NCT02824471, "Sickle Cell Disease Biofluid Chip Technology"). Surplus EDTA-anticoagulated whole blood collected for routine clinical lab work at the time of outpatient clinic visits was obtained from 16 consented subjects. Blood samples were packed in an insulated container on ice and shipped overnight to the laboratory for analysis. Subject samples were tested for adhesion and Hb composition within 24 hours of collection. Hb composition (fetal, HbF; sickle, HbS, and adult, HbA) was determined via High Performance Liquid Chromatography with a Bio-Rad Variant II Instrument (Bio-Rad, Montreal, QC, Canada) in the clinical core laboratory of University Hospitals Cleveland Medical Center (UHCMC). Clinical data were obtained from the electronic medical record for patients enrolled in the study from the adult SCD clinic at UHCMC, on dates contemporaneous with the blood sample collection.

Statistical Analysis: Statistical analyses were performed using Minitab. Data were tested for normality. One-way ANOVA test was performed to analyze the relationship of two independent groups. A two-way ANOVA. $p<0.05$ was chosen to indicate a significant difference. Weighted standard deviation of RBC density distributions is calculated with built-in function of MATLAB (The MathWorks, Inc). Receiver-operating curve was generated using MATLAB.[53] In addition to the area under the curve, sensitivity, specificity, positive and negative predicted value and accuracy values were calculated as follows: Sensitivity = TP / (TP + FN), Specificity = TN / (TN + FP), Negative predicted value = TN / (TN + FN), Positive predicted value = TP / (TP + FP) and

Accuracy = (TP + TN) / (TP + TN + FP + FN) (TP: true positive, TN: True negative, FP: False positive, FN: False negative).

REFERENCES

1. S. K. Ballas and N. Mohandas, *Microcirculation (New York, N.Y. : 1994)*, 2004, **11**, 209-225.
2. H. F. Bunn, *New England Journal of Medicine*, 1997, **337**, 762-769.
3. D. S. Chudwin, C. Papierniak, T. F. Lint and A. D. Korenblit, *Clinical Immunology and immunopathology*, 1994, **71**, 199-202.
4. N. Praljak, S. Iram, U. Goreke, G. Singh, A. Hill, U. A. Gurkan and M. Hinczewski, *PLOS Computational Biology*, 2021, **17**, e1008946.
5. M. Kim, Y. Alapan, A. Adhikari, J. A. Little and U. A. Gurkan, *Microcirculation (New York, N.Y. : 1994)*, 2017, **24**, e12374.
6. Y. Man, U. Goreke, E. Kucukal, A. Hill, R. An, S. Liu, A. Bode, A. Solis-Fuentes, L. V. Nayak, J. A. Little and U. A. Gurkan, *Blood Cells, Molecules, and Diseases*, 2020, 102424.
7. V. L. Lew and R. M. Bookchin, *Physiological Reviews*, 2005, **85**, 179-200.
8. V. L. Lew and T. Tiffert, *Frontiers in Physiology*, 2017, **8**.
9. S. Zheng, N. A. Krump, M. M. McKenna, Y. H. Li, A. Hannemann, L. J. Garrett, J. S. Gibson, D. M. Bodine and P. S. Low, *The Journal of Biological Chemistry*, 2019, **294**, 2519-2528.
10. P. Noomuna, M. Risinger, S. Zhou, K. Seu, Y. Man, R. An, D. A. Sheik, J. Wan, J. A. Little, U. A. Gurkan, F. M. Turrini, T. Kalfa and P. S. Low, *British Journal of Haematology*, 2020.
11. P. Sundd, M. T. Gladwin and E. M. Novelli, *Annual Review of Pathology*, 2019, **14**, 263-292.
12. K. Horiuchi, M. J. Stephens, K. Adachi, T. Asakura, E. Schwartz and K. Ohene-Frempong, *British Journal of Haematology*, 1993, **85**, 356-364.
13. M. G. Rakotoson, G. Di Liberto, E. Audureau, A. Habibi, C. Fauroux, S. Khorgami, A. Hulin, S. Loric, F. Noizat-Pirenne, F. Galacteros and P. Bartolucci, *Orphanet Journal of Rare Diseases*, 2015, **10**, 57.
14. V. L. Lew, O. E. Ortiz and R. M. Bookchin, *The Journal of Clinical Investigation*, 1997, **99**, 2727-2735.
15. P. Bartolucci, C. Brugnara, A. Teixeira-Pinto, S. Pissard, K. Moradkhani, H. Jouault and F. Galacteros, *Blood*, 2012, **120**, 3136-3141.
16. D. K. Kaul and M. E. Fabry, *Microcirculation (New York, N.Y. : 1994)*, 2004, **11**, 153-165.
17. J. A. Warth and D. L. Rucknagel, *Blood*, 1984, **64**, 507-515.
18. A. A. Kumar, M. R. Patton, J. W. Hennek, S. Y. R. Lee, G. D'Alesio-Spina, X. Yang, J. Kanter, S. S. Shevkoplyas, C. Brugnara and G. M. Whitesides, *Proceedings of the National Academy of Sciences*, 2014, **111**, 14864-14869.
19. P. T. Sharpe, *Methods of Cell Separation*, Elsevier, 1988.
20. T. P. Burg, M. Godin, S. M. Knudsen, W. Shen, G. Carlson, J. S. Foster, K. Babcock and S. R. Manalis, *Nature*, 2007, **446**, 1066-1069.

21. A. K. Bryan, V. C. Hecht, W. Shen, K. Payer, W. H. Grover and S. R. Manalis, *Lab on a Chip*, 2014, **14**, 569-576.
22. W. H. Grover, A. K. Bryan, M. Diez-Silva, S. Suresh, J. M. Higgins and S. R. Manalis, *Proceedings of the National Academy of Sciences*, 2011, **108**, 10992-10996.
23. J.-A. Ribeil, S. Hacein-Bey-Abina, E. Payen, A. Magnani, M. Semeraro, E. Magrin, L. Caccavelli, B. Neven, P. Bourget, W. El Nemer, P. Bartolucci, L. Weber, H. Puy, J.-F. Meritet, D. Grevent, Y. Beuzard, S. Chrétien, T. Lefebvre, R. W. Ross, O. Negre, G. Veres, L. Sandler, S. Soni, M. de Montalembert, S. Blanche, P. Leboulch and M. Cavazzana, *New England Journal of Medicine*, 2017, **376**, 848-855.
24. M. J. Van Osch, E. j. P. Vonken, M. A. Viergever, J. van der Grond and C. J. Bakker, *Magnetic Resonance in Medicine*, 2003, **49**, 1067-1076.
25. M. A. Gijs, F. Lacharme and U. Lehmann, *Chemical Reviews*, 2010, **110**, 1518-1563.
26. S. S. Shevkoplyas, A. C. Siegel, R. M. Westervelt, M. G. Prentiss and G. M. Whitesides, *Lab on a Chip*, 2007, **7**, 1294-1302.
27. H. C. Tekin, M. Cornaglia and M. A. Gijs, *Lab on a Chip*, 2013, **13**, 1053-1059.
28. K. A. Mirica, S. T. Phillips, C. R. Mace and G. M. Whitesides, *Journal of Agricultural and Food Chemistry*, 2010, **58**, 6565-6569.
29. K. A. Mirica, S. S. Shevkoplyas, S. T. Phillips, M. Gupta and G. M. Whitesides, *Journal of the American Chemical Society*, 2009, **131**, 10049-10058.
30. N. G. Durmus, H. C. Tekin, S. Guven, K. Sridhar, A. Arslan Yildiz, G. Calibasi, I. Ghiran, R. W. Davis, L. M. Steinmetz and U. Demirci, *Proceedings of the National Academy of Sciences*, 2015, **112**, E3661-E3668.
31. E. Danese, G. Lippi and M. Montagnana, *Journal of Thoracic Disease*, 2015, **7**, E402-411.
32. P. P. Priya and R. S. A, *Journal of Clinical and Diagnostic Research*, 2014, **8**, Fc01-03.
33. A. Dean, *Blood Groups and Red Cell Antigens*, 2004.
34. A. Sadaf, C. T. Quinn, J. B. Korpik, A. Pfeiffer, M. Reynaud, O. Niss, P. Malik, R. E. Ware, T. A. Kalfa and P. T. McGann, *Blood Cells Molecules and Diseases*, 2021, **90**, 102576.
35. Y. Ilboudo, P. Bartolucci, A. Rivera, J.-C. Sedzro, M. Beaudoin, M. Trudel, S. L. Alper, C. Brugnara, F. Galactéros and G. Lettre, *Blood Cells, Molecules, and Diseases*, 2017, **65**, 60-65.
36. V. Baudin, J. Pagnier, D. Labie, R. Girot and H. Wajcman, *Haematologia*, 1986, **19**, 177-184.
37. M. E. Fabry, J. G. Mears, P. Patel, K. Schaefer-Rego, L. D. Carmichael, G. Martinez and R. L. Nagel, *Blood*, 1984, **64**, 1042-1046.
38. Z. Yasin, S. Witting, M. B. Palascak, C. H. Joiner, D. L. Rucknagel and R. S. Franco, *Blood*, 2003, **102**, 365-370.
39. R. L. Nagel, R. M. Bookchin, J. Johnson, D. Labie, H. Wajcman, W. A. Isaac-Sodeye, G. R. Honig, G. Schilirò, J. H. Crookston and K. Matsutomo, *Proceedings of the National Academy of Sciences*, 1979, **76**, 670-672.
40. R. S. Franco, J. Lohmann, E. B. Silberstein, G. Mayfield-Pratt, M. Palascak, T. A. Nemeth, C. H. Joiner, M. Weiner and D. L. Rucknagel, *The Journal of Clinical Investigation*, 1998, **101**, 2730-2740.
41. S. Embury, M. Clark, G. Monroy and N. Mohandas, *The Journal of Clinical Investigation*, 1984, **73**, 116-123.

42. M. E. Fabry, A. C. Rybicki, S. M. Suzuka, M. C. Rahimy, R. Krishnamoorthy and R. L. Nagel, *Blood*, 2006, **108**, 1244-1244.
43. C. T. Quinn, E. P. Smith, S. Arbabi, P. K. Khera, C. J. Lindsell, O. Niss, C. H. Joiner, R. S. Franco and R. M. Cohen, *American Journal of Hematology*, 2016, **91**, 1195-1201.
44. G. L. Salvagno, F. Sanchis-Gomar, A. Picanza and G. Lippi, *Critical Reviews in Clinical Laboratory Sciences*, 2015, **52**, 86-105.
45. N. Li, H. Zhou and Q. Tang, *Disease Markers*, 2017, **2017**.
46. S. Jaiswal, P. Fontanillas, J. Flannick, A. Manning, P. V. Grauman, B. G. Mar, R. C. Lindsley, C. H. Mermel, N. Burtt, A. Chavez, J. M. Higgins, V. Moltchanov, F. C. Kuo, M. J. Kluk, B. Henderson, L. Kinnunen, H. A. Koistinen, C. Ladenvall, G. Getz, A. Correa, B. F. Banahan, S. Gabriel, S. Kathiresan, H. M. Stringham, M. I. McCarthy, M. Boehnke, J. Tuomilehto, C. Haiman, L. Groop, G. Atzmon, J. G. Wilson, D. Neuberg, D. Altshuler and B. L. Ebert, *New England Journal of Medicine*, 2014, **371**, 2488-2498.
47. J. L. Rapp, D. Tremblay, N. Alpert, W. Lieberman-Cribbin, J. Mascarenhas, E. Taioli and S. Ghaffari, *Journal of Medical Virology*, 2021, **93**, 4130-4132.
48. S. Kapoor, J. A. Little and L. H. Pecker, *Mayo Clinic Proceedings*, 2018, **93**, 1810-1824.
49. L. Thompson, B. Pinckney, S. Lu, M. Gregory, J. Tigges and I. Ghiran, *Journal of Visualized Experiments: Jove*, 2021.
50. N. Puluca, N. G. Durmus, S. Lee, N. Belbachir, F. X. Galdos, M. G. Ogut, R. Gupta, K.-i. Hirano, M. Krane, R. Lange, J. C. Wu, S. M. Wu and U. Demirci, *Advanced Biosystems*, 2020, **4**, 1900300.
51. A. Tocchio, N. G. Durmus, K. Sridhar, V. Mani, B. Coskun, R. El Assal and U. Demirci, *Advanced Materials*, 2018, **30**, 1705034.
52. J. R. Dillman, J. H. Ellis, R. H. Cohan, E. M. Caoili, H. K. Hussain, A. D. Campbell and P. J. Strouse, *Journal of Magnetic Resonance Imaging*, 2011, **34**, 917-920.
53. V. Martínez-Cagigal, ROC Curve, MATLAB Central File Exchange.

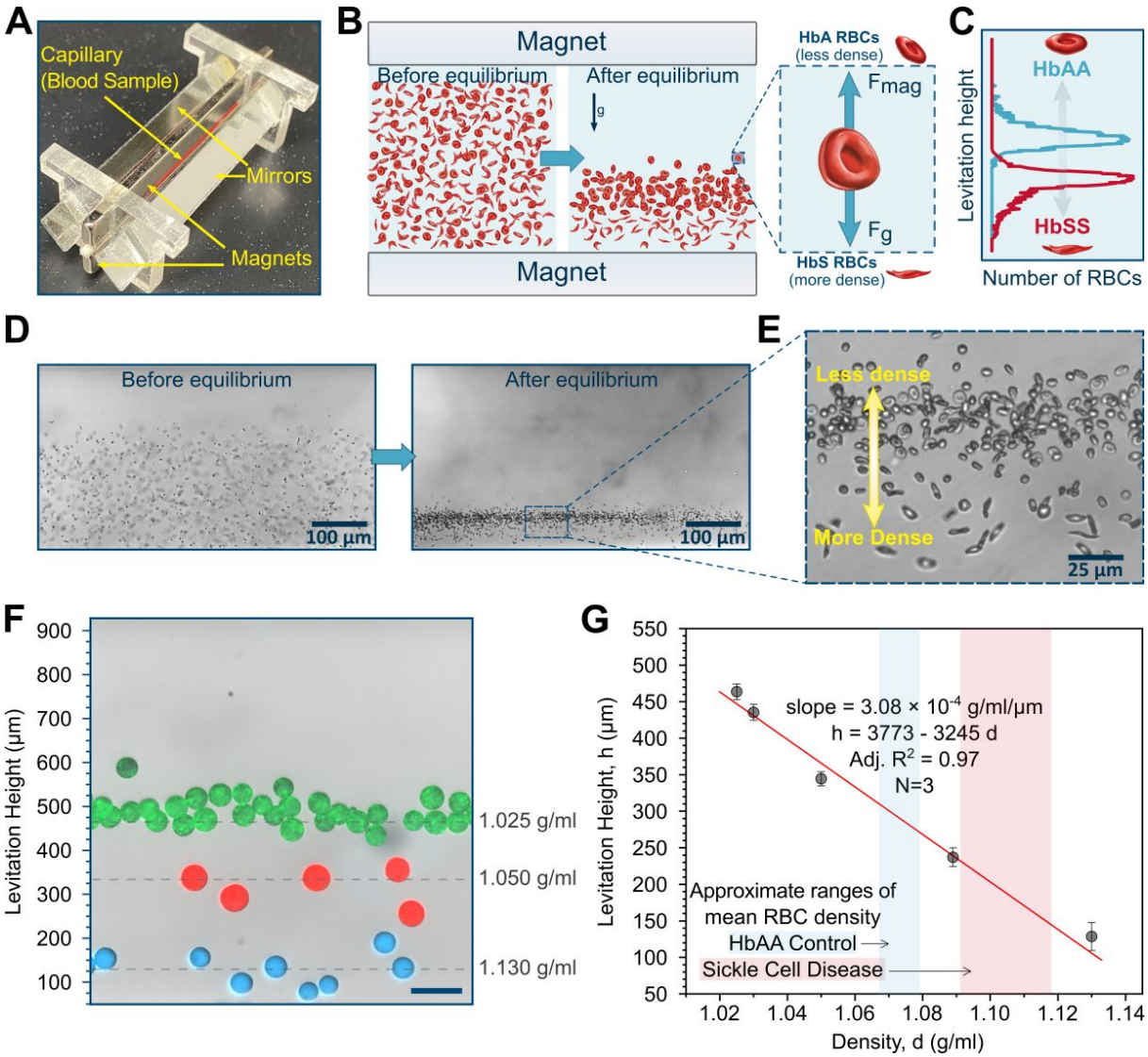

Figure 1. Microfluidic magnetic levitation-based red blood cell (RBC) density measurement assay at the single RBC level. **(A)** MagDense is composed of a microchannel placed between two permanent magnets. Tilted mirrors provide real-time imaging and efficient assessment of blood samples. **(B)** Diluted mixture of sickle and healthy RBCs are loaded into the microfluidic device and allowed to equilibrate under the effects of gravitational and magnetic levitation forces inside a paramagnetic medium. **(C)** Representative illustration of levitation height (µm, y-axis) versus cell number (x-axis) depicts distributions of denser, hemoglobin S containing RBCs (HbSS RBCs) compared to a normal control (HbAA RBCs). **(D)** Representative microscopic images of levitating RBCs before and after equilibrium. **(E)** Based on precisely measured levitation height and density of cells in levitation state, the density of HbS containing RBCs and HbA containing normal RBCs can be accurately analyzed. Less dense HbA RBCs levitate higher, while the denser HbS RBCs levitate lower in the channel. **(F)** Representative levitation image of density-based separation of reference beads within the MagDense device. *Scale bar is 100 µm* **(G)** The relationship between the bead density and levitation heights in 30 mM paramagnetic medium. Linear fitting curve of each data point provides a standard function for measuring densities of particles. The slope of the curve represents the amount of density change per micrometer levitation

height, which is converted to density change per pixel of microscope image. 3.08×10^{-4} g/ml/μm corresponds to 0.98×10^{-4} g/ml/pixel under 20x objective.

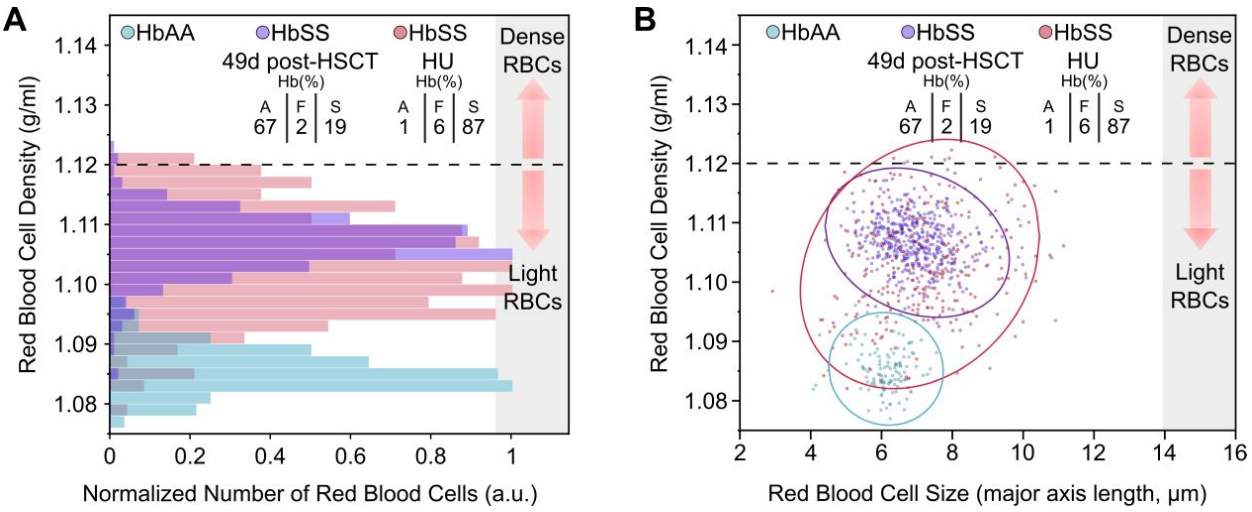

Figure 2. Size and density analysis of red blood cells (RBCs) at a single cell level provides RBC classification by cluster analysis with respect to RBC density and size. (A) The histogram plots for density distributions of an HbAA control subject with no known hemoglobinopathy (light blue) and from two subjects with homozygous sickle cell disease; a subject who receives hydroxyurea (red) and a subject who recently received hematopoietic stem cell transplant (HSCT, purple). HbAA RBCs have a narrower distribution of both density and size, compared to HbSS RBCs. **(B)** Scatter plots of cell density versus cell size (major axis length) for HbAA and HbSS RBCs with confidence ellipses (95% coverage). Confidence ellipse of HU subject with high HbS and HbF shows greater heterogeneity, probably due to presence of both dehydration resistant cells and cells with higher density.

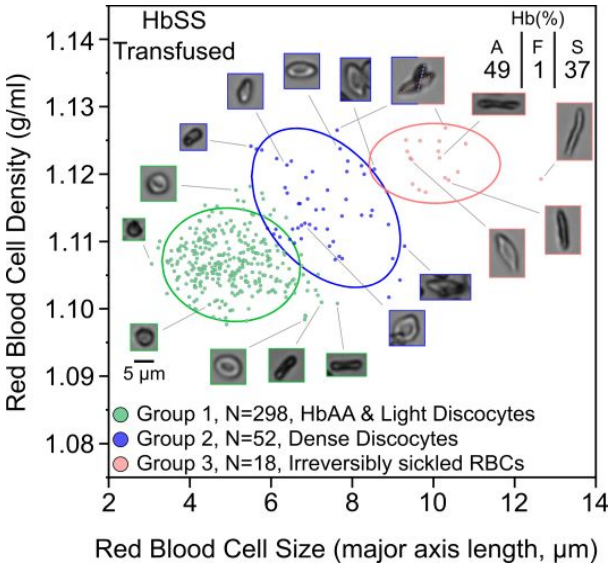

Figure 3. Three groups of red blood cells (RBCs) revealed by clustering of scatter plots from a transfused homozygous sickle cell disease (HbSS SCD) subject. HbSS SCD subjects cannot produce HbAA containing RBCs and blood transfusions are needed to replace sickle RBCs with HbAA RBCs. Some of sickle RBCs may be dehydration resistant, while some of them become irreversibly sickled after cycles of hemoglobin polymerization. Scatter plots of individual subjects can be post processed to explore different RBC clusters of distinct size and density. Clusters were identified with agglomerative hierarchical clustering method. Representative images of RBCs with different shapes were depicted as inset figures next to their corresponding dots.

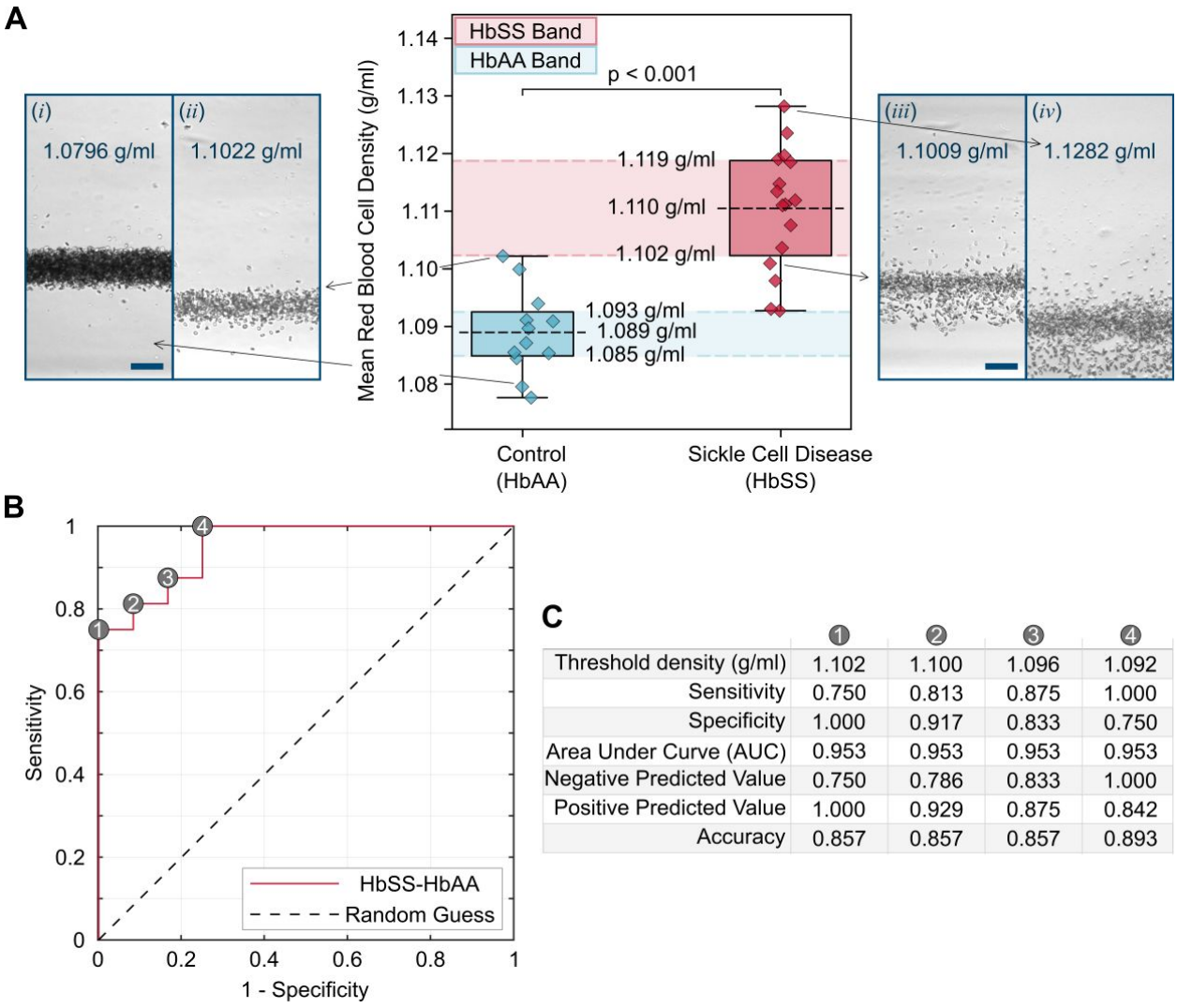

	❶	❷	❸	❹
Threshold density (g/ml)	1.102	1.100	1.096	1.092
Sensitivity	0.750	0.813	0.875	1.000
Specificity	1.000	0.917	0.833	0.750
Area Under Curve (AUC)	0.953	0.953	0.953	0.953
Negative Predicted Value	0.750	0.786	0.833	1.000
Positive Predicted Value	1.000	0.929	0.875	0.842
Accuracy	0.857	0.857	0.857	0.893

Figure 4. RBC density, measured by MagDense, is significantly greater (p<0.001, ANOVA) for subjects with sickle cell disease (SCD) (HbSS, N=16) compared with non-sickle control (HbAA, N=12). (A) Bands represent anticipated range for the RBC density for each group and are defined as interquartile ranges. Blue dashed rectangle represents the HbAA band, which is the anticipated results for the assay following fully curative therapy, with complete reversal of the abnormal red cell phenotype in SCD. *Scale bars are 80 μm.* **(B)** Receiver operating curve (ROC) demonstrate sensitivity and 1-specificity for differentiation of HbSS from HbAA subjects based on mean RBC density. Enumerated bullets on the curve denotes four different thresholds of mean RBC density. The first threshold represents the lower boundary of the HbSS band. The second threshold has the minimum distance to unity among four. **(C)** ROC analysis outputs are tabulated for each threshold shown in the previous panel.

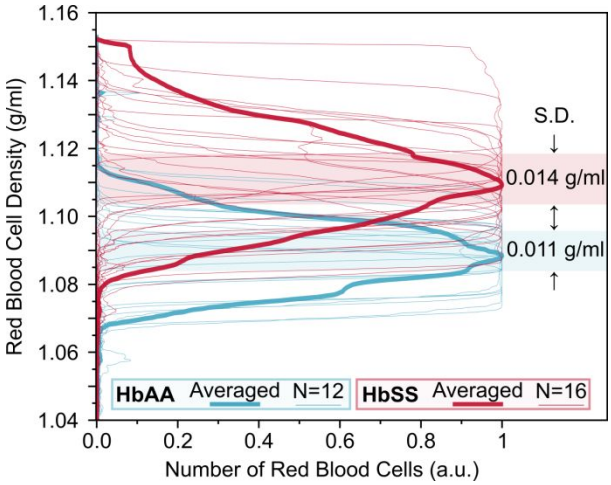

Figure 5. Dispersion of red blood cell (RBC) density from the mean can be assessed by MagDense with high resolution. The weighted standard deviation of the averaged RBC density curves was found to be greater in HbSS, compared to HbAA. Red lines represent subjects with sickle cell disease (SCD) and blue lines represent non-sickle, control subjects. Thin lines depict the RBC density distribution for individuals and thick lines show the averaged RBC distribution of each group of subjects.

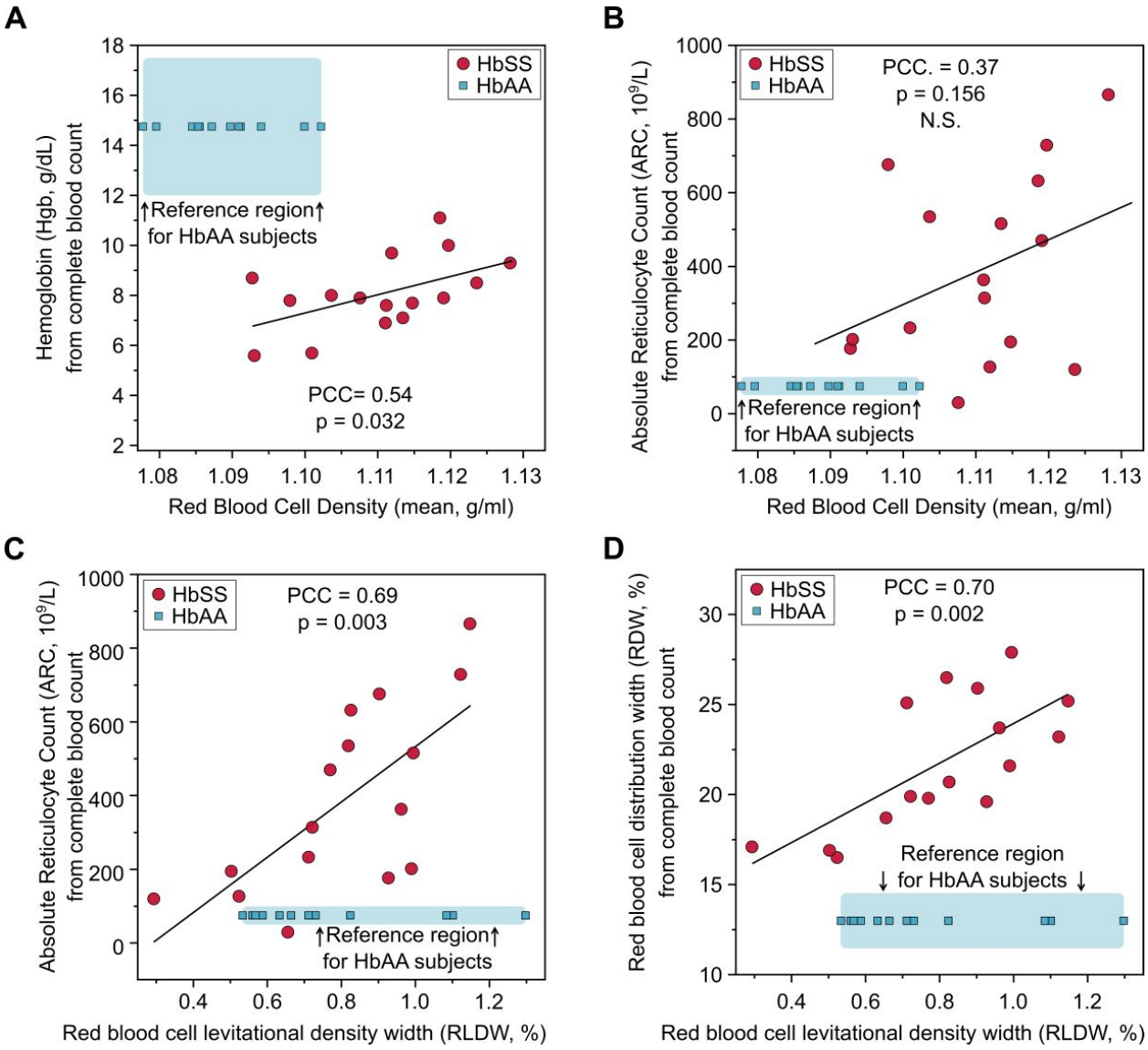

Figure 6. Red blood cell (RBC) density parameters, mean RBC density and RBC levitational density width (RLDW) are positively related with clinical laboratory test results in sickle cell disease (SCD). (A) Hemoglobin is one of the most abundant protein in RBCs. The hemoglobin concentration from the clinical laboratory results is associated with mean RBC density (PCC=0.54, p=0.032, Pearson correlation and linear regression). **(B)** Absolute reticulocyte count (ARC) is considered as a disease severity marker in SCD. There was no significant association between ARC and mean RBC density, however, **(C)** there was a significant relation of increased ARC with increased RLDW (PCC=0.69, p=0.003, Pearson correlation and linear regression), which implies greater intra-patient RBC density heterogeneity as measured by MagDense platform. **(D)** The RDW as measured by central clinical laboratory and RLDW was significantly and positively related (PCC=0.70, p=0.002, Pearson correlation and linear regression). *Blue boxes represent likely regions for HbAA subjects in each plot.*

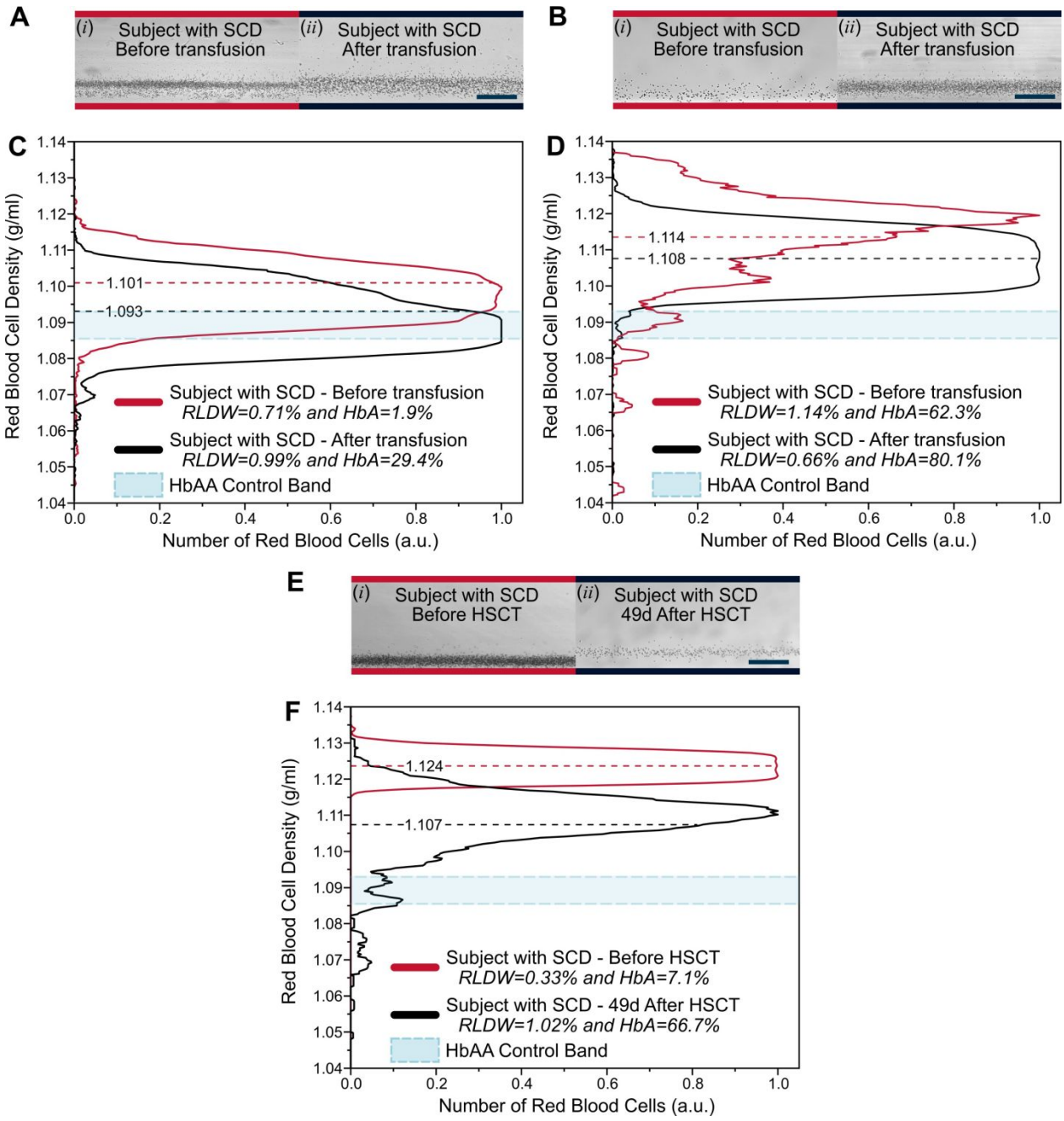

Figure 7. MagDense magnetic levitation-based red blood cell (RBC) density measurement assay at the single RBC level can be used to predict patient response to the clinical interventions. (A-B) Levitational height change after blood transfusion treatment can be observed visually from microscope images of RBCs within the MagDense channel. Shown are representative microscope images of red blood cells within MagDense capillary (*i*) before and (*ii*) after the SCD subjects receive blood transfusion. **(C-D)** Mean RBC density of samples from individuals with sickle cell disease (SCD) approaches to HbAA control range following a transfusion treatment. **(E)** Levitational height (*i*) before and (*ii*) after hematopoietic stem cell transplantation (HSCT). HSCT is a curative therapy **(F)** Mean RBC density decreased from 1.124 g/ml to 1.107 g/ml following HSCT, along with an increase in RLDW. *Scale bars are 300 μm.*